Off-fault plasticity favors the arrest of dynamic ruptures on strength heterogeneity : Two-dimensional cases

Sébastien Hok, Michel Campillo, Fabrice Cotton, Pascal Favreau, Ioan Ionescu

GEOPHYSICAL RESEARCH LETTERS, VOL. 37, L02306, doi:10.1029/2009GL041888, 2010

Off-fault plasticity favors the arrest of dynamic ruptures on strength heterogeneity: Two-dimensional cases

S. Hok,[1,2] M. Campillo,[1] F. Cotton,[1] P. Favreau,[3] and I. Ionescu[4]

Received 23 November 2009; accepted 23 December 2009; published 30 January 2010.

[1] We study the effects of a plastic behavior of the volume around the fault on in-plane and anti-plane 2D rupture dynamics. Both rupture modes exhibit similar answer to off-fault yielding, in terms of modification of the kinematics of the rupture front, and in terms of energy lost outside the fault plane. We then compare the ability of the rupture to propagate through a barrier on the interface. The plastic behavior, responsible for a linear increase of the global fracture energy during dynamic crack growth, enhances the rupture front sensitivity to a static resistance increase on the fault. Consequently, the rupture arrest is more easily provoked in heterogeneous models that include a plastic yielding, even with relatively small variations of frictional resistance along the fault plane. **Citation:** Hok, S., M. Campillo, F. Cotton, P. Favreau, and I. Ionescu (2010), Off-fault plasticity favors the arrest of dynamic ruptures on strength heterogeneity: Two-dimensional cases, *Geophys. Res. Lett.*, *37*, L02306, doi:10.1029/2009GL041888.

1. Introduction

[2] A plastic mechanical behavior is expected from the damaged medium that is likely to encompass the faults up to several tens of meters [e.g., *Chester et al.*, 2004; *Dor et al.*, 2006]. Off-fault cracking has been also identified as a possible mechanism to explain slip profiles linear trends that show off from natural earthquakes [*Manighetti et al.*, 2004]. Since a damaged medium contains secondary faults, and low cohesion cataclasite layers, it cannot bear high deviatoric stresses without breaking. Hence, the elastic response of the material next to the main fault plane is limited, as fracturing or re-activation of pre-existing fractures can occur when it experiences the high transient stresses driven by the propagating rupture. Many numerical studies showed that off-fault cracking was induced by the main fault rupture process [e.g., *Yamashita*, 2000; *Poliakov et al.*, 2002; *Dalguer et al.*, 2003; *Ando and Yamashita*, 2007].

[3] As cracking outside the fault consumes fracture energy, its simultaneity with the rupture process on the main fault plane modifies the dynamic energy balance, which controls the propagation of the crack. For instance, *Templeton and Rice* [2008] found that off-fault plasticity was delaying the supershear transition. Previously, *Andrews* [2005] showed that the total fracture energy, including the energy dissipated inelastically, is increasing linearly with rupture propagation distance.

[4] Other recent numerical studies addressed different cases, such as bimaterial medium [e.g., *Ben-Zion and Shi*, 2005; *Duan*, 2008b], or low velocity zone [*Duan*, 2008a]. But these studies considered spatially homogeneous friction properties rather than properties that change spatially along the fault plane. However, it is reasonable to consider that, in reality, the rupture front does not propagate on a smooth fault, and that a spatial heterogeneity of friction parameters is necessary to explain many characteristics of earthquake rupture and particularly its arrest.

[5] We limit our analysis to the 2D case. This is a convenient way to investigate the propagation process at the local scale of the rupture front, but it might not be relevant to consider a finite barrier dimension along the propagation direction while dealing with a 2D case. Consequently, we will consider the simple case where the static friction exhibits a step at a certain location of the fault. This can be seen as a barrier, if the rupture stops, or as an increase of the fracture energy, if the rupture goes on.

[6] A few studies of off-fault cracking considered 3D geometries [*Dalguer et al.*, 2003; *Ma*, 2008]. In 2D, only the in-plane case has been studied. Our paper presents results for the anti-plane 2D case, and checks the consistency between anti-plane and in-plane results. All the computations presented have been done for both modes.

2. Numerical Modeling and Homogeneous Fault Validation Tests

[7] For the dynamic rupture calculations, we use the numerical code introduced by *Favreau and Archuleta* [2003]. The finite-difference scheme is 4th order in space, 2nd order in time, and solves the elasto-dynamic equations in the velocity-stress formulation on a staggered-grid. The code has been modified to include a limit to the maximum resolved shear stress inside the bulk, as if micro-ruptures were occurring. The elasto-plastic limit follows a Mohr-Coulomb criterion as a function of the confining stress and of the cohesion of the material. Below the limit, the medium behaves as a perfect elastic body, and above it, the energy is lost for off-fault rupturing. This formulation has been described and used by *Andrews* [2005]. For the method validation, we used almost the same parameter set to compute homogeneous cases, except the time step that was chosen 4 times smaller. The main difference comes from the use of a slip-weakening constitutive law instead of a time-weakening law, but they have been shown to be similar in the case of off-fault yielding [*Duan and Day*,

[1]Laboratoire de Géophysique Interne et Tectonophysique, Université Joseph Fourier, CNRS, Grenoble, France.
[2]Now at National Research Institute for Earth Science and Disaster Prevention, Tsukuba, Japan.
[3]Institut de Physique du Globe de Paris, CNRS, Paris, France.
[4]Laboratoire des Propriétés Mécaniques et Thermodynamiques des Matériaux, Institut Galilée, Université Paris 13, CNRS, Villetaneuse, France.

0094-8276/10/2009GL041888$05.00

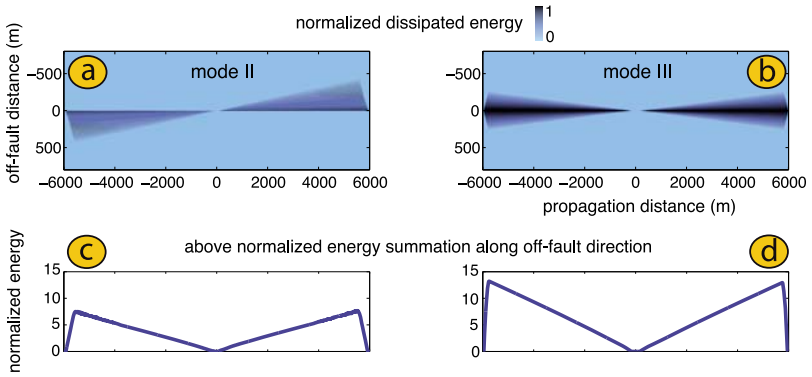

Figure 1. (top) Location and normalized amplitude of the off-fault plastic energy lost dynamically, for both (a) in-plane (left-lateral strike-slip fault) and (b) anti-plane cases. The mode II geometry shows an asymmetrical damage pattern, localized on the extensional side of the fault, whereas in the mode III geometry, the damage zone spreads on both sides of the fault. For both modes, the width of off-fault yielding zone increases linearly with the rupture propagation distance. (bottom) Total energy dissipated in the medium as a function of the propagation distance of the crack tip. (c and d) In both cases, the energy lost outside the fault increases linearly with propagation distance.

2008]. We used a 2 m grid step, and a 0.0792 ms time step. The medium density is set to 2700 kg.m^{-3}, the P wave velocity is 5196 m.s^{-1} and the S wave velocity is 3000 m.s^{-1}. On the fault, the normal stress is 50 MPa, and the initial shear stress is 10 MPa. Note that the other compressive stress values, parallel to the fault plane, are identical to the fault normal stress, which implies that the principal stress direction is 45° with respect to the fault plane. The friction law has a critical slip distance of 0.035 m, the static friction stress is 25 MPa (friction coefficient is 0.5), while the dynamic friction stress is 0 MPa. Off the fault, the plasticity surface is defined with a friction coefficient of 0.75, and a zero cohesion. To study the interaction with the barrier, we needed to increase S value from 1.5 to 2 (S is the ratio between the static stress increase needed to rupture and the stress drop) by setting the initial shear stress to 8.5 MPa. We also used a four times larger slip-weakening distance d_c set to 0.14m. This modification is discussed later in the paper. Non-zero values of the cohesion have also been used to decrease the off-fault yielding effect.

[8] Following *Favreau et al.* [2002], the initiation of the rupture is obtained spontaneously by prescribing a gaussian-shaped velocity perturbation (center point slip at 2 m/s) at 20 points at the center of the nucleation zone, at t = 0. The rupture initiation zone is located at the center of the fault, and spans over 200 m (just above the critical crack length for the given parameters and same value used by *Andrews* [2005]). The small initial perturbation grows dynamically on this patch, where the static resistance is equal to the initial loading stress, and finally proceeds spontaneously into a dynamic crack that is able to propagate outside the nucleation zone.

[9] We checked that in mode II, considering the homogeneous properties, we retrieved the same slip velocity limitation, the same asymmetric lateral extension of the plasticity after 2 km of propagation and the same linear dependency of the off-fault fracture energy with rupture length as found by *Andrews* [2005].

[10] In mode III, we obtained very similar saturation effects on the kinematics. Anti-plane rupture with off-fault yielding also exhibits a slight reduction of the rupture speed, as well as a strong limitation of the maximum slipping velocity, clearly associated with a saturation of the slip gradient at the crack tip. With the same model parameters, the spreading rate of the damage zone width is similar to mode II, reaching about 500 m after 6 km of propagation, while it reaches 450 m in mode II (Figures 1b and 1a). However, the damage zone spreads now on both side of the fault, as could be inferred from 3D calculations [*Dalguer et al.*, 2003; *Ma*, 2008].

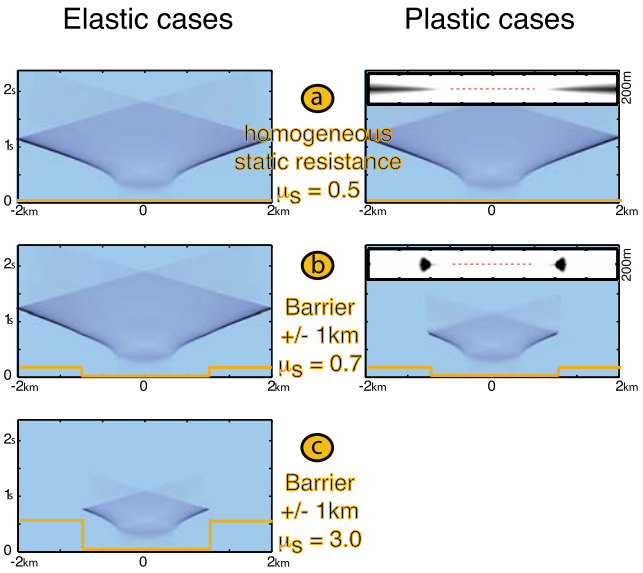

Figure 2. Space and time rupture propagation for (left) elastic and (right) plastic models (mode III). (a) The homogeneous case shows the slightly slower rupture velocity when accounting for off-fault yielding. (b) The impact of the barrier on the rupture front depends on its strength: (c) a higher barrier stops the rupture. The plasticity enhances the barrier strength: the propagation is now stopped, where it was not even slowed down in the elastic model (Figure 2b). μ_s is the static friction coefficient. In the plastic cases, top subplot shows the total off-fault yielding spatial extension. Please refer to Figures S1 and S2 of the auxiliary material for additional values of μ_s, similar mode II case, and shear stress space/time evolution.

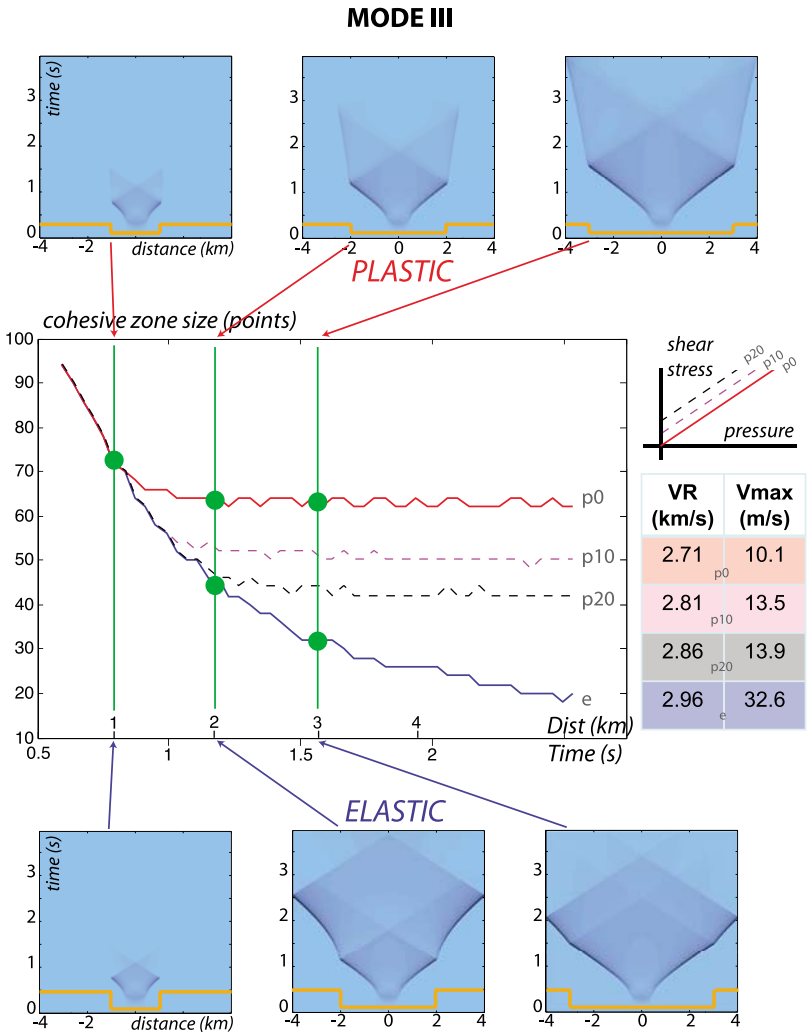

Figure 3. Evolution of the cohesive zone size as crack lengthens for homogeneous cases (constant μ_s). Central plot shows how it shrinks in an elastic case (blue) and three plastic case (red - pink - black). These 3 models only differs by their plasticity surface's cohesion value, respectively 0 - 10 - 20 MPa. The lower the cohesion, the higher the off-fault yielding effect (see right hand side table). Blue cartoons show the impact on the rupture propagation of a μ_s increase (yellow line), located at various distance from the initiation point (see also green line in middle plot). μ_s jumps from 0.50 to 0.67 in the plastic cases (top) and from 0.50 to 2.00 in the elastic cases (bottom). The rupture velocity after the change reveals the impact of the barrier. While it is different for each different location in the elastic cases, it remains similar in the plastic cases. It demonstrate the stabilization of the energy balance by off-fault plastic yielding. The auxiliary material Figure S3 provides the mode II case (similar curves).

[11] An important result is that, for both 2D cases, the plastic energy dissipated inside the bulk surrounding the fault is linearly increasing with the rupture length. Moreover, the quantity of energy lost in plastic processes is of the same order for both rupture modes (Figures 1c and 1d).

3. Fracture Energy Change on the Main Fault Plane

[12] When sticking to the homogeneous cases, the effect of the plastic dissipation seems mainly limited to the trailing edge of cohesive zone, as a consequence of the rapid stress drop on the main fault. The global fracture energy increase, due to off-fault cracking, never leads to the spontaneous arrest of the crack propagation, as far as we computed. This is because the rupture front propagates steadily at its terminal velocity on a smooth fault, leading to very little interaction with off-fault processes. To investigate this assumption, we study the rupture behavior in presence of both off-fault plastic yielding and a static resistance change.

[13] The static resistance change has to be small, so that the main fault remains the weakest plane. That is the reason why the constitutive law on the fault has been changed to a higher fracture energy and lower loading stress. This modification decreases the crack instability (increase of both S and d_c) before the strength change, compared to the original values of *Andrews* [2005]. We found that this combination of parameters, used for the homogeneous case study, leads to a too unstable rupture (for instance, the terminal velocity is reached very quickly), that is not likely to be stopped only by a small change of friction on the main rupture plane (considering that our fault is very smooth before the friction change, hence far from the critical state when reaching this point).

[14] Without any heterogeneity (Figure 2a), as said before, the crack propagates more slowly in the plastic case than in the elastic case. When introducing a change of static resistance at 1 km from the nucleation point, one can see, in elastic cases, that the effect on the crack is correlated to the strength of the barrier (μ_s), which determines the on-fault fracture energy. The off-fault plastic yielding changes dramatically the behavior of the rupture front at the resistance change: Figure 2b shows that the rupture front can now be stopped by barriers that were not even able to slow down the propagation in the elastic case (please refer to Figures S1 and S2 of the auxiliary material to see the complete set of parameters tested).[1] Note that, with off-fault plasticity, the crack does not stop abruptly at the barrier, but rather dies inside the higher resistance zone. This type of arrest is similar to what happens with strengthening barriers [*Voisin et al.*, 2002].

[15] Equivalently, in the elastic case, the effect of a barrier can be linked to its closeness from the nucleation point of the rupture. As the energy balance of a crack depends on its length, as discussed in the scope of the κ parameter by *Madariaga and Olsen* [2000] for 3D cracks stability, the location of the barrier determines its effect on the rupture propagation. A good proxy for the energy state of the rupture front is the width of the cohesive zone. In homogeneous slip-weakening models, it should scale inversely with the energy increase of the crack during its growth [*Andrews*, 2004], while in plastic slip-weakening models, the cohesive zone size is prevented from decreasing [*Duan and Day*, 2008]. The limit size, as well as the maximum slip-velocity, depends on the relative part of energy that is lost dynamically outside the fault. This can be seen in Figure 3, which also illustrates the consequences on the crack propagation (please refer to Figure S3 to compare with mode II). While in the elastic case, a smaller cohesive zone, meaning more available energy, is related with the ability to jump the barriers, in the off-fault yielding case, the effect of the barrier remains the same whatever the rupture size (same rupture velocity in the barrier area) since the cohesive zone does not shrink anymore. Figure 3 also shows that considering a more realistic non-zero value for the cohesion parameter does not change this conclusion. The limit size is different, but it still saturates. Hence, in the plastic case, the condition in which the rupture is stopped by a given barrier is independent of the size of the rupture, contrary to what happens in the elastic case. This result shows that off-fault yielding modifies strongly the rupture ability to propagate through a variable resistance fault and suggest a larger sensitivity of fault friction properties in presence of off-fault plasticity.

4. Conclusions

[16] We show that mode II and mode III rupture interact similarly with dynamic off-fault damage. Not only the impact on the rupture front kinematics, but also the energy that is lost off the fault, are comparable. Our computations then show how off-fault plastic yielding changes the rupture ability to propagate along a variable resistance fault. This is deduced from letting the rupture propagate through a barrier (static friction coefficient increase). We see that a rupture embedded in a medium where the stress yields, stops much more easily when it encounters a barrier than in elastic cases. Part of the rupture energy is dissipated outside the fault, and the crack cannot break through the barriers. This may explain why, in reality, rupture seems to be stopped by relatively slight changes of properties, while in elastic modeling, very strong barriers are required to arrest large cracks. If the stresses are limited outside the fault by some form of damage process, as they are in the plastic calculations, one can understand that spontaneous arrest of the rupture can occur on smooth faults with modest lateral variations of friction properties.

[17] **Acknowledgments.** We thank the reviewers for useful remarks and their suggestions to improve the presentation of this manuscript. All the computations presented in this paper were performed at the Service Commun de Calcul Intensif de l'Observatoire de Grenoble (SCCI). The initial part of this work has been funded by an INSU Program ACI Risques Naturels et Changements Climatiques. M.C. and F.C. benefited from the support of Institut Universitaire de France.

References

Ando, R., and T. Yamashita (2007), Effects of mesoscopic-scale fault structure on dynamic earthquake ruptures: Dynamic formation of geometrical complexity of earthquake faults, *J. Geophys. Res.*, *112*, B09303, doi:10.1029/2006JB004612.

Andrews, D. J. (2004), Rupture models with dynamically determined breakdown displacement, *Bull. Seismol. Soc. Am.*, *94*(3), 769–775.

Andrews, D. J. (2005), Rupture dynamics with energy loss outside the slip zone, *J. Geophys. Res.*, *110*, B01307, doi:10.1029/2004JB003191.

Ben-Zion, Y., and Z. Shi (2005), Dynamic rupture on a material interface with spontaneaous generation of plastic strain in the bulk, *Earth Planet. Sci. Lett.*, *236*, 486–496.

Chester, F. M., J. S. Chester, D. L. Kirschner, S. E. Schulz, and J. P. Evans (2004), Structure of large-displacement, strike-slip fault zones in the brittle continental crust, in *Rheology and Deformation in the Lithosphere at Continental Margins*, edited by G. D. Karner et al., pp. 223–260, Columbia Univ. Press, New York.

Dalguer, L. A., K. Irikura, and J. D. Riera (2003), Simulation of tensile crack generation by three-dimensional dynamic shear rupture propagation during an earthquake, *J. Geophys. Res.*, *108*(B3), 2144, doi:10.1029/2001JB001738.

Dor, O., Y. Ben-Zion, T. K. Rockwell, and J. Brune (2006), Pulverized rocks in the Mojave section of the San Andreas fault zone, *Earth Planet. Sci. Lett.*, *245*, 642–654.

Duan, B. (2008a), Effects of low-velocity fault zones on dynamic ruptures with nonelastic off-fault response, *Geophys. Res. Lett.*, *35*, L04307, doi:10.1029/2008GL033171.

Duan, B. (2008b), Asymmetric off-fault damage generated by bilateral ruptures along a bimaterial interface, *Geophys. Res. Lett.*, *35*, L14306, doi:10.1029/2008GL034797.

Duan, B., and S. M. Day (2008), Inelastic strain distribution and seismic radiation from rupture of a fault kink, *J. Geophys. Res.*, *113*, B12311, doi:10.1029/2008JB005847.

Favreau, P., and R. J. Archuleta (2003), Direct seismic energy modeling and application to the 1979 Imperial Valley earthquake, *Geophys. Res. Lett.*, *30*(5), 1198, doi:10.1029/2002GL015968.

Favreau, P., M. Campillo, and I. R. Ionescu (2002), Initiation of shear instability in three-dimensional elastodynamics, *J. Geophys. Res.*, *107*(B7), 2147, doi:10.1029/2001JB000448.

Ma, S. (2008), A physical model for widespread near-surface and fault zone damage induced by earthquakes, *Geochem. Geophys. Geosyst.*, *9*, Q11009, doi:10.1029/2008GC002231.

Madariaga, R., and K. B. Olsen (2000), Criticality of rupture dynamics in 3-D, *Pure Appl. Geophys.*, *157*, 1981–2001.

Manighetti, I., G. King, and C. G. Sammis (2004), The role of off-fault damage in the evolution of normal faults, *Earth Planet. Sci. Lett.*, *217*, 399–408, doi:10.1016/S0012-821X(03)00601-0.

Poliakov, A. N. B., R. Dmowska, and J. R. Rice (2002), Dynamic shear rupture interactions with fault bends and off-axis secondary faulting, *J. Geophys. Res.*, *107*(B11), 2295, doi:10.1029/2001JB000572.

Templeton, E. L., and J. R. Rice (2008), Off-fault plasticity and earthquake rupture dynamics: 1. Dry materials or neglect of fluid pressure changes, *J. Geophys. Res.*, *113*, B09306, doi:10.1029/2007JB005529.

[1] Auxiliary materials are available in the HTML. doi:10.1029/2009GL041888.

Voisin, C., I. Ionescu, and M. Campillo (2002), Crack growth resistance and dynamic rupture arrest under slip dependent friction, *Phys. Earth. Planet. Inter.*, *131*, 279–294, doi:10.1016/S0031-9201(02)00054-7.

Yamashita, T. (2000), Generation of microcracks by dynamic shear rupture and its effects on rupture growth and elastic wave radiation, *Geophys. J. Int.*, *143*, 395–406.

M. Campillo and F. Cotton, Laboratoire de Géophysique Interne et Tectonophysique, Maison des Géosciences, Université Joseph Fourier, BP 53, F-38041 Grenoble CEDEX 9, France.

P. Favreau, Institut de Physique du Globe de Paris, 4 place Jussieu, Case 89, F-75252 Paris CEDEX 05, France.

S. Hok, National Research Institute for Earth Science and Disaster Prevention, 3-1 Tennodai, Tsukuba, Ibaraki 305-0006, Japan. (shok@bosai.go.jp)

I. Ionescu, Laboratoire des Propriétés Mécaniques et Thermodynamiques des Matériaux, Institut Galilée, Université Paris 13, 99 Ave. Jean-Baptiste Clément, F-93430 Villetaneuse CEDEX, France.